

Article

The Deltah Lab, a New Multidisciplinary European Facility to Support the H₂ Distribution & Storage Economy

Sara Stelitano ^{1,*}, Alberto Rullo ¹, Luigi Piredda ¹, Elisabetta Mecozzi ¹, Luigi Di Vito ¹, Raffaele Giuseppe Agostino ², Raffaele Filosa ², Vincenzo Formoso ², Giuseppe Conte ² and Alfonso Policicchio ²

¹ Rina Consulting-Centro Sviluppo Materiali, Via Di Castel Romano 100, 00128 Roma, Italy; alberto.rullo@rina.org (A.R.); luigi.piredda@rina.org (L.P.); elisabetta.mecozzi@rina.org (E.M.); luigi.divito@rina.org (L.D.V.)

² Department of Physics, Università della Calabria, via Pietro Bucci, 87036 Arcavacata di Rende, Italy; raffaele.agostino@fis.unical.it (R.G.A.); raffaele.filosa@fis.unical.it (R.F.); vincenzo.formoso@fis.unical.it (V.F.); giuseppe.conte@unical.it (G.C.); alfonso.policicchio@fis.unical.it (A.P.)

* Correspondence: sara.stelitano@rina.org

Abstract: The target for European decarbonization encourages the use of renewable energy sources and H₂ is considered the link in the global energy system transformation. So, research studies are numerous, but only few facilities can test materials and components for H₂ storage. This work offers a brief review of H₂ storage methods and presents the preliminary results obtained in a new facility. Slow strain rate and fatigue life tests were performed in H₂ at 80 MPa on specimens and a tank of AISI 4145, respectively. Besides, the storage capacity at 30 MPa of a solid-state system, they were evaluated on kg scale by adsorption test. The results have shown the H₂ influence on mechanical properties of the steel. The adsorption test showed a gain of 26% at 12 MPa in H₂ storage with respect to the empty condition. All samples have been characterized by complementary techniques in order to connect the H₂ effect with material properties.

Keywords: hydrogen facility; hydrogen economy; hydrogen embrittlement; hydrogen storage; hydrogen sorption



Citation: Stelitano, S.; Rullo, A.; Piredda, L.; Mecozzi, E.; Di Vito, L.; Agostino, R.G.; Filosa, R.; Formoso, V.; Conte, G.; Policicchio, A. The Deltah Lab, a New Multidisciplinary European Facility to Support the H₂ Distribution & Storage Economy. *Appl. Sci.* **2021**, *11*, 3272. <https://doi.org/10.3390/app11073272>

Academic Editor: Andrea Frazzica

Received: 19 February 2021

Accepted: 23 March 2021

Published: 6 April 2021

Publisher's Note: MDPI stays neutral with regard to jurisdictional claims in published maps and institutional affiliations.



Copyright: © 2021 by the authors. Licensee MDPI, Basel, Switzerland. This article is an open access article distributed under the terms and conditions of the Creative Commons Attribution (CC BY) license (<https://creativecommons.org/licenses/by/4.0/>).

1. Introduction

The 2018/2001/EC Directive of the European Parliament [1] sets the objective of reaching at least 32% of the EU's final energy consumption through renewable energy sources (RES) by 2030. The RES drawback is their intermittence, which must be balanced for electric grid stability purposes through long term and large capacity storage. This entails a challenge in terms of developing and matching suitable fuel/energy source, generation, storage, transmission, distribution, and customer-side requirements to balance and integrate RES with current electricity grids. In this context, some energy storage systems have been proposed, which include pumped hydro-storage, compressed-air storage, battery energy storage, superconducting energy storage, thermal energy storage, and chemical energy storage technologies [2]. Reviews of the different energy storage technologies are given by Aneke [2] and by Koochi-Fayegh [3] which highlight their advantages and disadvantages in real-life applications. Among different storage systems, chemical energy storage technology represents one of the main explored because it can convert RES surplus electricity into gaseous energy carriers, mainly H₂ and CH₄, which can be transformed back into electricity, integrated into a power-to-gas system or used as fuel [4–7]. H₂ can be directly used as a fuel in the stationary sector to provide power and in the mobile sector, using fuel cells [8]. In the mobile sector, H₂ can improve energy efficiency in transport and participates in climate change mitigation [9,10]. To date, increasingly efficient means of H₂ transport have been developed, in particular, there are now cars with autonomy ranging

from 1 kg/100 km (Hyundai ix35) to 0.76 kg/100 km (Toyota Mirai) with 0 kg/km CO₂ emissions [11]. H₂ has the highest energy density per unit mass of any fuel, but being the lightest and lowest density element, it is hardly stored and requires more volume for a given amount of energy [12]. The development of H₂ as a reliable energy vector is strongly associated with the performance and the level of safety of the components of the supply chain [13,14].

For this reason, accomplishing efficient storage is crucial to address the H₂ economy, so its storage is one of the principal topics of research. H₂ economy development needs both mobile and stationary storage systems [15,16].

Regarding stationary applications, H₂ storage problems of weight and volume are not as much persuasive compared to mobile applications. Despite this, the greatest technical barriers for stationary systems are represented by inadequate materials and few standards, contrary to mobile systems that are well-defined by the U.S. Department of Energy. The department requires a gravimetric/volumetric capacity, defined as the usable quantity of H₂ deliverable to the fuel cells divided by the total mass/volume of the complete storage system, of 2.2 kWh/kg and 1.7 kWh/l for stationary and mobile systems, respectively [17]. To achieve these parameters, different storage techniques have been developed: gas compression (cGH₂), liquefaction (lH₂), cryo-compressed (CcH₂), liquid (LSMs), and solid-state materials (SSMs), which involve the H₂ interaction with the bulk (Chemisorption—Chem) or the surface (Physisorption—Phys) of materials [18,19]. cGH₂ is the most popular storage solution for both stationary and mobile applications, which requires expensive tanks, due to considerations on materials, geometry and mechanical properties, compression, and fast filling resulting in energy expenditure [12]. lH₂ permits to store more H₂ than cGH₂, but it requires even higher energy expenditure for liquefaction of the gas and the insulation of the vessel, necessary to avoid the boiling of H₂, with a lost energy content estimated as 40% in contrasts to 10% of energy lost for cGH₂. The CcH₂ combines the properties of cGH₂ and lH₂ systems to minimize the boil-off rate and maintain a high energy density. The CcH₂ systems use insulated tanks that can accept cryogenic temperatures (20 K), as lH₂, and high pressure (at least 30 MPa) at ambient temperature, as cGH₂. The higher resistance to the high pressure of the tank allows greater increases in pressure before H₂ has to be boiled, so there is a reduction in boiling loss retaining a system energy density like cGH₂. For many years, LSMs and SSMs have been considered as an alternative [20–23]. They have good storage capacities, but present low temperature for Phys, high desorption temperature for Chem, complex kinetics and thermodynamics of the processes. There is no general solution for the storage method, this must be carefully designed and selected to address specific applications depending on geometry characteristics, working conditions, storage equipment, technical performances, costs, and safety requirements. In this scenario, materials for H₂ components and infrastructures are a critical theme to guarantee reliability and safety, so their characterization is fundamental to evaluate the H₂ effect on them in specific conditions. In particular, the effect of pressure and temperature on material properties must be investigated to address loading conditions close to the operation. Among the tests, slow strain rate tests (SSRTs) are considered necessary to investigate the effect of H₂ on ductility, fracture mechanics and fatigue tests are fundamental at both the design and verification stage of components; while adsorption-desorption tests are essential to evaluate the storage performance of a SSMs system. Besides, several complementary techniques are considered essential to analyze the H₂ effects on materials, particularly in steel types and SSMs. Generally, to characterize the crack formation, conventional fractographic methods, e.g., scanning (SEM) and transmission (TEM) electron spectroscopy, were used [24], but in the last years, many different techniques were adopted such as X-ray computed microtomography. Micro-tomography is one method to reconstruct complex 3D structures of the cracks, which has already been applied to observe stress corrosion cracking in steel [25,26] and in aluminium alloys [27,28]. Regarding SSMs, porosimetry and SEM are the most used techniques to characterize the texture and morphology of adsorbent materials, which represent an indication of material capacity to storage H₂ [29,30].

H₂ represents one of the most attractive energy carriers, it has many applications such as stationary, mobile, backup, or speciality. In order to make H₂ of common use, it is necessary to make its production, distribution, and application safe, reliable, and commercial. A number of technical problems need to be solved before H₂ can be used as a common energy carrier. The problems involve the technology of production, storage, transmission, distribution, and ultimate application in a broad field of methods of end-use. Besides, it is evident that there are several problems related to H₂ use and its interaction with materials. In this context, there are several studies and investigations in the scientific sector, but only few facilities are able to test and validate the materials and components for H₂ storage and distribution in view of real application.

This paper offers a brief review of H₂ storage methods and an extensive presentation of a new testing facility with its preliminary results in the field of H₂ storage. The work highlights the lab capabilities to analyze and evaluate the H₂ effects on materials and so on their storage capability, both with mechanical tests, on materials and components, and adsorbent materials, connecting these storage abilities with morphological, structural, and chemical properties of materials. Thank to these skills, the facility represents an interdisciplinary laboratory able to help the research and industrial sector to develop and validate materials and components for the new hydrogen economy. Then, the present work shows the results of SSRT and fatigue life tests conducted in the H₂ environment at high pressure on AISI 4145 steel specimens and a tank, respectively, and of an adsorption-desorption test on an SSM system, highlighting the correlation between storage performance and materials properties.

2. Hydrogen Storage Systems

At the state of the art, the most common ways to store H₂ are cGH₂, lH₂, CcH₂, and SSMs, as reported in Table 1, where gravimetric and volumetric capacity values, at specific pressure and temperature, pros and cons of each storage method are listed [20,31].

Table 1. Hydrogen storage systems comparison.

Storage Method	Gravimetric Capacity [wt%]	Volumetric Capacity [kgH ₂ /m ³]	T [K]	P [MPa]	Pros	Cons
CGH ₂	6	< 40	RT	70	High efficiency, convenient, mature technology	Expensive cylinder and the immature technology of fast filling.
lH ₂	8	70	20	0.1	High liquid density and storage efficiency	Large consume of energy and time, low temperature, boil-off
CcH ₂	~5	~40	20	30	Low boil-off	High costs
SSMs -Phys	2	20	77	10	Highly porous, high uptake of H ₂ and specific surface areas, fully reversible	Very low storage temperature
SSMs -Chem	15	150	RT	2	High safety, high purity of H ₂ good reversible cycle performance, large volume of H ₂ density	Absorbing impurities, reducing the H ₂ capacity and the lifetime of tank

The important criteria for an H₂ storage system are the gravimetric capacity (the amount of H₂ adsorbed per unit mass, expressed as kg H₂ kg⁻¹ or as a weight percentage (wt.%), which decrease with the pressure increases), the volumetric capacity (the amount of H₂ adsorbed per unit volume, as g H₂ m⁻³, which increases with the pressure increases), the pressure and the temperature. Gravimetric and volumetric capacities influence the

weight and the volume of a storage tank, respectively, while pressure and temperature determine the operation condition influencing, besides the geometry of the vessel, the costs and safety of the full system. cGH_2 is the most deep-rooted storage solution in different sectors since the end of the 19th century so that regulations, codes and several standards have been set up for different applications. Considering the storage applications, pressure vessels are typically used in the industrial stationary field as storage and buffering and in the mobility field for on-board power supply and storage in refueling stations. This method requires deepened studies on materials and geometries to design the more appropriate and safe tanks useful to use in transportation, stationary and portable systems. The storage pressure affects the thickness of the container walls, the size and weight of the containers, the choice of materials, and the costs. Currently, the cGH_2 can be stored in four different types of pressure vessels (Type I to Type IV), that can be pressurized up to 25, 35, or 70 MPa [32]. Type I metallic (generally steel or metal alloys) pressure vessel is mostly used for industrial applications with a pressure of 20–30 MPa, but it is only able to store about 1 wt% of H_2 . These are also used in refueling station where the storage of large volumes at medium pressure (about 20 MPa) and high and very high pressure (about 50 and 100 MPa) are foreseen to quickly refuel the vehicles. These are designed for large supplies of H_2 (up to 8 tons/day and more) with the need for large storage volumes. In Type II, the cylindrical metal (mostly steel or aluminum) part of the vessel is wrapped with fiber resin composite, while the Type III and Type IV are fully composite wrapped vessels, in which the composite is plastic or carbon fibers embedded in a polymer matrix and the inner liner is metallic (generally aluminium) or plastic, respectively. Comparing the different vessel types, Type I and Type II cannot be used in the vehicles owing to low gravimetric H_2 storage density [33] and H_2 embrittlement (HE) effect, which affects the metal (steel or metal alloy) of which they are made [34]. HE occurs when metals become brittle because of the diffusion of H_2 into the material. The embrittlement degree is affected both by the amount of H_2 absorbed and the microstructure of the material. Consequently, there is a loss of ductility and a reduction of load-bearing capability of the metal due to the absorption of H_2 atoms or molecules by it. The effect of HE is that components crack and fracture at stresses less than the yield strength of the metal. The HE is a dangerous phenomenon depending on different factors such as gas pressure, temperature, and loading conditions, so the effects of HE on materials properties are fundamental for their possible application with high-pressure H_2 gas [35,36]. Differently, Type III and Type IV types are largely used in the automotive sector due to their low weight, where H_2 is stored at a pressure of 35 MPa (buses, trains, goods movement) and 70 MPa (passenger vehicles and heavy transport). High pressures are required to achieve high energy density and the need to reduce the transportable weight pushes towards lightweight composite solutions [37]. Despite its diffusion and the presence of different standards on the design of materials and vessels, the cGH_2 storage still requires significant improvements in terms of technical and practical applications. In metal vessels, there is the necessity of a deeper study of fatigue life and the HE effects. In the case of composite vessels, of a more recent conception, several issues still need to be explored: gas permeation, thermo-mechanical performance, fiber breaks, delamination, matrix cracking, liner blistering, fire-resistant, inspection and re-testing criteria, and the development of techniques using low-cost fibers. Another conventional storage method is based on the H_2 liquefaction at 20 K, which has high storage efficiency. Compared to cGH_2 , lH_2 allows higher densities (70 kg/m^3 , approximately double compared to H_2 stored in gaseous form at a pressure of 70 MPa and triple compared to storage at 35 MPa). H_2 liquefies at ambient pressure and a temperature of 20 K, therefore the containers for the transport and storage of liquefied H_2 must have very strict thermal insulation requirements. The simplest liquefaction process is the Linde cycle or Joule–Thompson expansion cycle. Liquid H_2 containers have reached a high degree of development and are generally designed with a spherical or cylindrical shape because they are the ones that allow a smaller surface space for the same volume. From a technical point of view, vessel design methods are described on ISO 21009 and ISO 13985. The vessels used for lH_2 are composed of an

inner vessel and an external protective jacket. The thermal conductivity between the two layers can be minimized by applying perlite or wrapping it with layers of aluminum films. So, the vessel design must consider, in addition to the topics in common with the vessels for cGH₂, the low temperature which significantly affect mechanical properties causing expansion and contractions phenomena. [32,38]. Ultimately, the storage of liquid H₂, while representing a commercial solution and having the advantage of allowing a greater energy density than other solutions, is time-consuming, energy-intensive, and affected by gas loss and so is mainly used in specific sectors, such as space programmes, in the medical or chemical industry, and for gas transportation by tracks. CcH₂ storage method combines the properties of both cGH₂ and IH₂ systems to reduce the boil-off loss of IH₂ and maintain a high energy density. The cCH₂ vessel must be able to store H₂ at 20 K and high pressure, at least 30 MPa, allowing greater pressure increases before H₂ has to be boiled off. This significantly extends the time before starting evaporative losses and thus increase storage autonomy [32]. The storage methods described present some limitations: the low energy density by volume, which requires a large pressure vessel; the costs of the pressure vessel; time and energy consuming for compression and/or liquefaction; safety of the vessel if it is used in densely populated areas [12]. Storage of H₂ in LSMs and SSMs is considered as an alternative safest method [22,23]. Specifically, different solid materials have been proposed as new H₂ storage systems, including metal-organic frameworks (MOFs) [39], zeolites [40], metal hydrides [41], polymers [42], hollow glass microspheres [43], and carbon-based materials [44]. Depending on the type of H₂-material interaction, the storage method is defined as physisorption, when the interaction depends on physical forces such as in the case of MOF or carbon-based materials, or chemisorption when there are chemical forces between H₂ and material such as in the case of metal hydrides [45]. The main advantages of the physisorption process are high energy efficiency and fast adsorption/desorption cycles, but it generally requires cryogenic temperatures (typically 77 K) and high pressures due to weak van der Waals forces involved (4–10 kJ·mol⁻¹), which limit its commercial development. The essential characteristics for an ideal material for physisorption are a high surface area available per unit volume of the adsorbent, which increases the quantities of the adsorbed H₂, and the characteristic binding energy of the H₂ molecule with the material [46]. Instead, the chemisorption has stronger binding energy (50–100 kJ·mol⁻¹) and allows to absorb a larger amount of gas but it is not a reversible process and requires high temperatures to release the adsorbed gas. SSMs represent one of the alternative storage methods, but there are some drawbacks still to overcome: low temperature in the case of physisorption materials, high temperature for the desorption of chemisorption materials, the kinetics and thermodynamics of the processes. To allow H₂ to be stored in SSMs at ambient temperature with adequate storage density, different approaches have been considered: improving H₂ storage capacities at ambient temperature for physisorption materials; improving kinetics and thermodynamics; as well as developing new materials and catalysts with high storage capacities at lower temperatures for chemisorption systems [47].

3. ΔH Test Lab

Hydrogen influences the mechanical properties of materials, in particular, fracture resistance and fatigue performances. Several activities are ongoing in these topics, but in Europe, there are few laboratories equipped with instruments to test materials and components in the H₂ environment combining the effect of high pressure and temperature. In this context, the idea to build a new H₂ facility was born to characterize materials and components for H₂ storage. The design and set-up of the lab were a quite challenging task, because of high pressure and the large range of temperatures that had to be considered. A brief description of the philosophy followed for the setup of the ΔH lab is here reported, together with the main results of the first activities carried out.

General Description

The ΔH lab was built in the frame of the “EOMAT” project (PON03PE_00092_1) funded within of the Italian National Operational Programme ‘Research and Competitiveness’ 2014–2017 [48], thanks to a cooperation between Rina Consulting—CSM SpA and University of Calabria. The entire construction has been classified as an explosion-proof zone 2 according to the ATEX 2014/34/UE and 99/92/CE directives and so, all the relevant equipment inside the bunker is adequate to this classification. The facility comprises a first H_2 production-compression-distribution room, three testing rooms and an external gas storage area. (Figure 1a). The compressor and the test installations are connected to a distribution system composed of high-pressure stainless-steel piping, control valves, pressure and temperature sensors, back-pressure valves, and a burner for venting. The lab presents two separated gas lines (Figure 1b): the first line at high pressure (100 MPa), dedicated to small- and full-scale tests and supplied by ultrapure H_2 bundle of bottles, and a second line at 30 MPa, dedicated to tests on SSMs and supplied by an H_2 generator. Every line is fed by a specific air-driven booster compression unit, a three-stage and a single-stage compressor for the first and the second line, respectively, so that both testing facilities can simultaneously work with both lines safely. Each room is equipped with gas sensors connected to the lab control systems to operate in a safe condition. In normal operation, the laboratory can run automatically, and the tests are controlled by an operator from a control room near the structure, besides there is the option to accomplish the tests from remote in order to work in full safety.

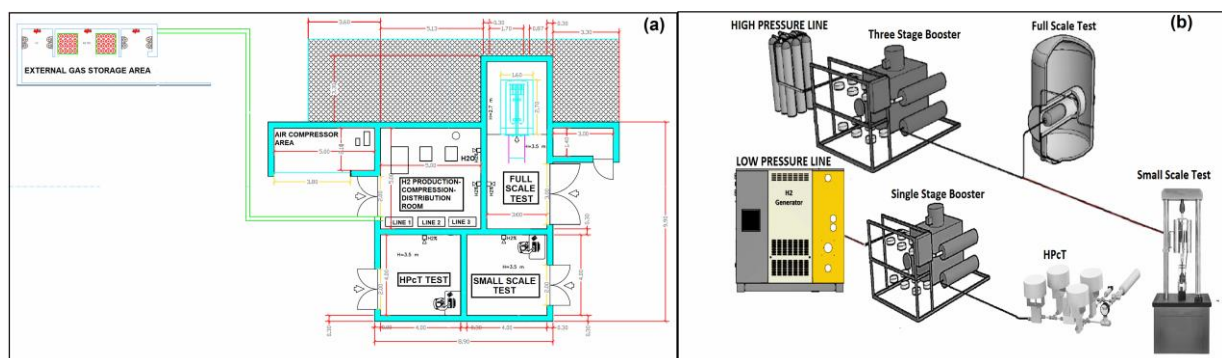


Figure 1. (a) ΔH Lab map, (b) ΔH Lab gas lines.

The lab is dedicated to test of materials and components for gas storage (mainly H_2) and distribution by three equipment:

A small-scale testing device mainly devoted to characterization (e.g., slow strain rate, tensile, toughness, fracture mechanics, and fatigue tests) of materials (steel, metal alloys and composites) with different strength corresponding to the machine and load cell characteristics. This permit to characterize the materials in an H_2 environment, in a pressure range (ΔP) of 0–100 MPa and temperature range (ΔT) of 283–423 K by a servo-hydraulic machine (Figure 2a) equipped with a 100 kN load cell. For fracture tests, crack propagation can be monitored using an alternate current potential drop system.

A full-scale device to assess the performance of materials (steel, metal alloys and composites) and components close to service conditions. This mainly consists of compression and decompression cycles of samples (e.g., bolt-load compact) components (e.g., tubes, cylinders, valves, etc.) for H_2 storage and distribution in a ΔP of 0–100 MPa. The component under test is inserted inside (Figure 2b) an inert security chamber of 2500 L filled with N_2 at 1 MPa.

A SSMs testing equipment, named high-pressure-concentration-temperature (HPcT), permits to evaluate the sorption/desorption capacity of a SSM in quantity from 500 g to 20 kg in a ΔP of 0–30 MPa and ΔT of 77–473 K using tanks from 1 to 50 litre. The HPcT (Figure 2c) system is an apparatus for continuous H_2 -sorption measurements in

dynamic conditions. A mass flow controller and a series of pneumatic valves allow to feed and released the gas inside the SSM and so to check, by a dedicated control and analysis software, the ability of the tested materials to ab/adsorb and desorb H_2 .

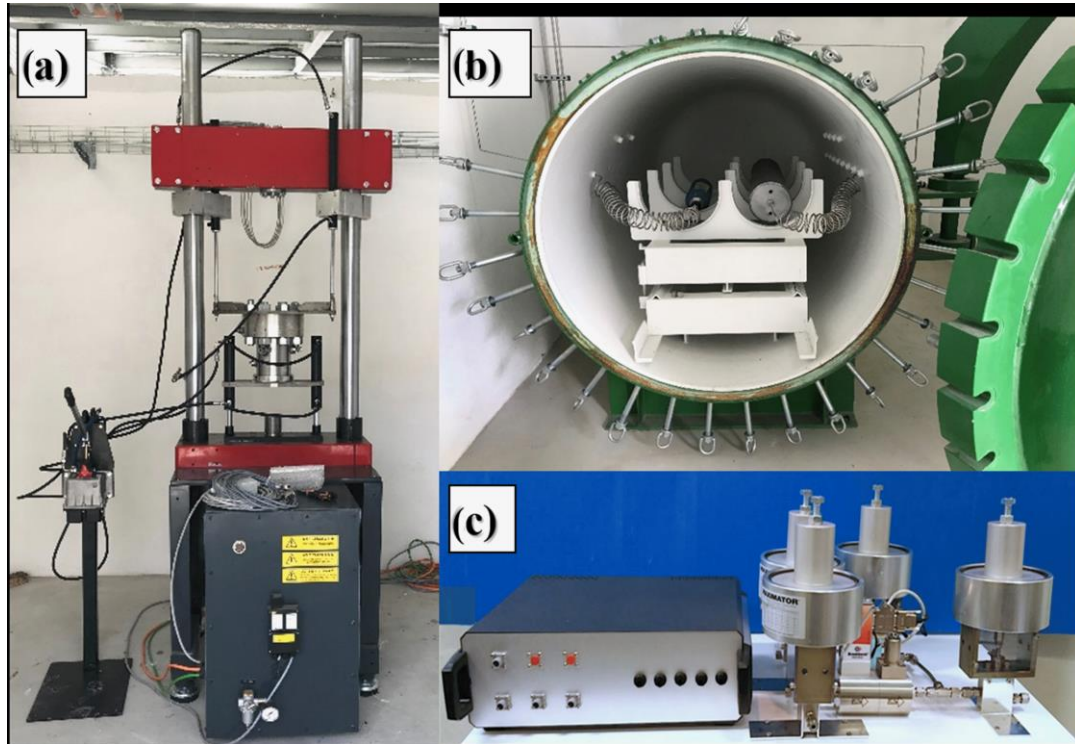


Figure 2. ΔH Lab test: (a) Servo-hydraulic machine for small scale tests, (b) Inert security chamber for full scale tests, and (c) High-Pressure-Concentration-temperature (HPCT) for adsorption tests.

4. Materials and Methods

4.1. Materials

The material under investigation was AISI 4145 steel in the form of cylindrical vessels with a very high level of cleanliness from inclusions and a microstructure consisting mainly of homogeneous martensite through the thickness. The chemical composition of the material was 0.47C-0.25Si-1.10Mn-1.10Cr-0.33Mo (mass %) and the average Vickers hardness, HV was 340. The 0.2% offset yield and tensile strength were found to be 827 and 1034 MPa, respectively. The specimens were extracted from the shell section of the cylindrical pressure vessel along the longitudinal direction and machined in a smooth specimen with an overall length of 70 mm, gauge section length of 25.4 mm, and diameter of 3.81 mm, according to NACE TM0198.

The full-scale test was conducted on an AISI 4145 vessel, containing an intentionally machined defect. A defect represents a preferential point for the initiation of potential fatigue cracks, to this purpose, the vessel was prepared preliminarily with two internal notches of a defined geometry. The notches are positioned at 0° and 180° , with a radius 0.15 mm, length of 20 mm, and depth of 1 and 1.5 mm, respectively. Then, the vessel was treated internally with solvent degreasing to remove residues of paraffinic hydrocarbons used in processing.

The sample for the SSM test was composed of a commercial AA 6061 T6 aluminum alloy cylinder, with a capacity of 1 L and a maximum working pressure of 30 MPa, filled with a commercial activated carbon (NUCHAR SA-1500). The NUCHAR SA-1500 was previously characterized in its morphology, porous properties, and small-scale adsorption capacity, showing a specific surface area of $2219 \text{ m}^2/\text{g}$, a micropore volume of $0.67 \text{ cm}^3/\text{g}$ with an average pore width of 0.95 nm, and an adsorption capacity at 294 K of 0.35 wt% [49].

4.2. Testing

The testing campaign was performed in the ΔH lab to investigate the H_2 effect on mechanical properties of materials and components for H_2 storage.

The small-scale tests were represented by SSRTs which are considered a most useful experiment for the valuation of the susceptibility of materials to H_2 gas, as confirmed by two ASTM STP collections [50,51] and several related publications [52]. The SSRT experimental procedure is defined by the ASTM G129, and it represents a tensile experiment led using a slow strain rate ($<10^{-5} \text{ s}^{-1}$), while the specimen is exposed to the environment of interest.

Tests were conducted at ambient temperature in an H_2 environment at a pressure of 80 MPa and, for comparison, in an inert environment (N_2) at the same pressure with a strain rate was 10^{-6} s^{-1} , corresponding to a crosshead speed of $0.025 \mu\text{m/s}$.

In order to evaluate the performance of a vessel in an H_2 environment, a fatigue full scale test was executed by pressure cycling at room temperature an AISI 4145 steel tank at ΔP of 5–45 MPa. In order to monitor the progress of an eventual crack, strain gauges were installed on the external surface of the cylinder close to the defects.

After mechanical tests, in order to observe morphology changes and the H_2 effects on the samples, SEM and tomography images of samples were recorded using an FEI Quanta FEG 200, a field emission scanning electron microscope (ESEM) with an electron beam of 20 keV, and a STAR's μ Tomo experimental station, composed by a microfocus X-ray tube as source, with focal spot size $5 \mu\text{m}$ (at 4 W) and high power, which allows continuous operations with a maximum output of 150 kV and 500 μA , and by a CMOS flat-panel sensor as detector, respectively.

An H_2 adsorption test on SSM was performed by the HPcT apparatus on a tank filled with 512 g of NUCHAR SA-1500. A reference test was carried out by comparing the amount of H_2 that, under the same pressure and temperature conditions, was introduced into a reservoir with a fixed volume.

5. Results

5.1. Slow Strain Rate Test

The tests performed in H_2 and N_2 show an evident influence of H_2 , as it is possible to note in Figure 3.



Figure 3. (a) Image of AISI 4145 smooth specimen tested in H_2 ; (b) Image of AISI 4145 smooth specimen tested in N_2 .

The sample tested in an H_2 environment (Figure 3a) does not show any elongation and reduction of the area typical of a ductile failure, suggesting a brittle fracture mode. The sample tested in N_2 environment at the same pressure (Figure 3b) shows a typical cup-and-cone fracture representative of ductile behavior. Figure 4 shows the stress vs. elongation curves recorded during the the two SSR tests in the H_2 and N_2 environment, respectively.

The curves show that the minimum elongation, before failure in the H_2 , is more than half the elongation of the sample in a N_2 environment likewise, as reported by Matsunaga et al. for a similar Cr-Mo steel [53] and contrary to carbon and austenitic steels [54,55]. This behavior suggests a brittle fracture mode and so the presence of HE effect, with an index value of 39%, calculated according to Briottet et al. [53]. The fracture surface analyses (Figure 5) confirm the presence of a brittle fracture. The fracture propagation path follows a 45° angle to the sample axis (Figure 5a,b), indicating that the cracking propagation follows the path of maximum shear deformation, similar to Cr-Mo steels in

different works [54] and austenitic steels [55,56]. The SEM images highlight the presence of secondary cracks (Figure 5c,d), indicating the high susceptibility of the external surfaces of the specimen.

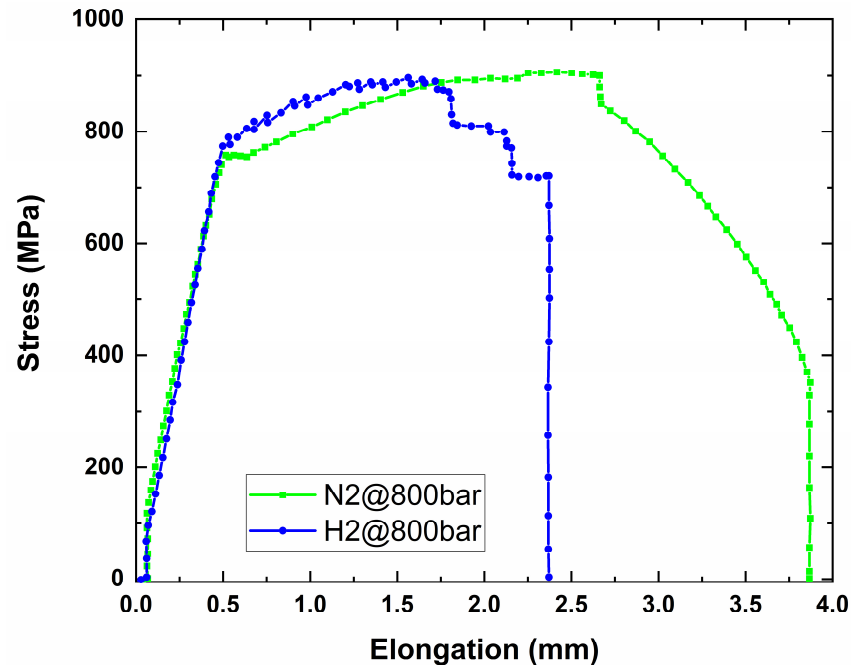


Figure 4. Stress vs. elongation curve in H_2 environment and in N_2 environment.

From the micrographs of Figure 5c,d, a mainly brittle fracture surface is visible. Specifically, the fracture at the center of the specimen has both transgranular and intergranular zones. Microductile areas are also present. On the contrary, the sample tested in N_2 shows a typical ductile fracture (Figure 6) with the characteristic cone shape, such as reported in other studies for different steels [54–57].

A confirmation of the presence of a secondary crack is given by tomography images. Figure 7 shows as in the hydrogenated specimen, the traction caused the creation of lateral microfractures, parallel to the sliding planes of the specimen, an evident element of the fragile fracture. On the contrary, the lateral profile of the specimen loaded in N_2 does not show micro-fractures, because in presence of a ductile fracture, the specimen tends to stretch without the creation of cracks on the lateral surface.

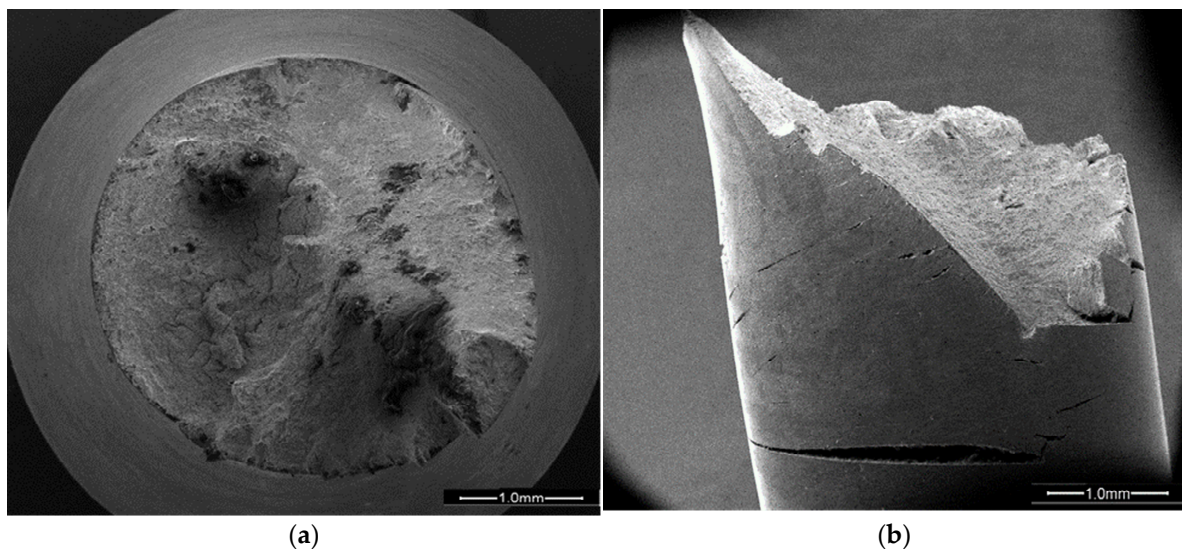


Figure 5. Cont.

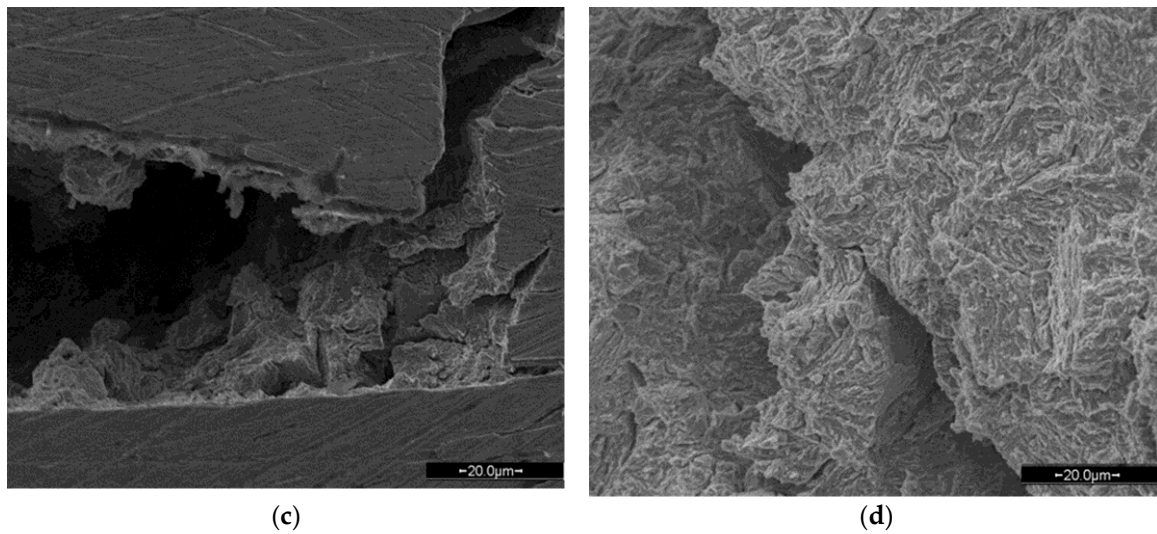


Figure 5. (a) SEM fracture surface of SSR sample tested in H₂. (b) Lateral Image of SEM fracture surface of SSR sample tested in H₂. (c) Secondary crack image of SEM fracture surface of SSR sample tested in H₂. (d) Surface of the crack of SEM fracture surface of SSR sample tested in H₂.

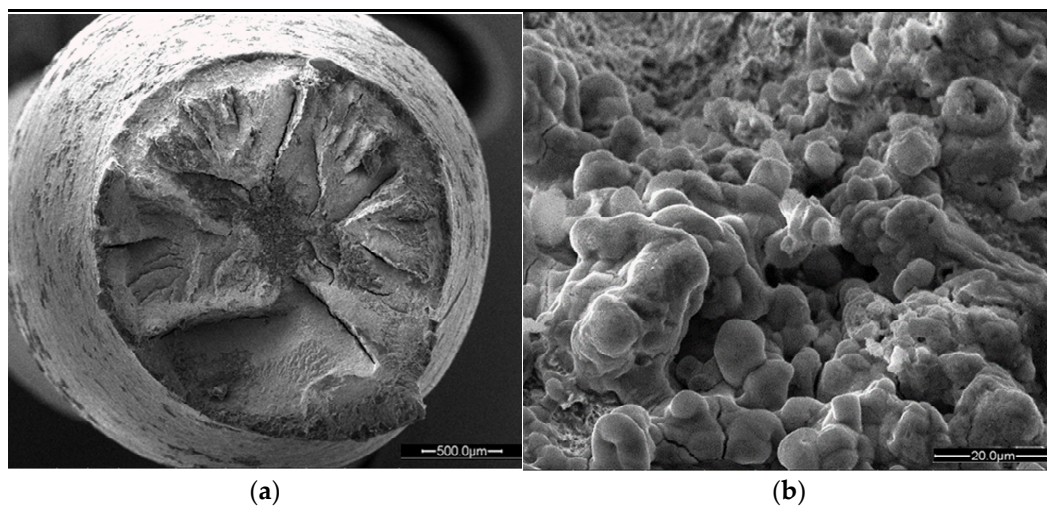


Figure 6. (a) SEM fracture surface area of SSR sample tested in N₂; (b) SEM image of the surface of SSR sample tested in N₂.

5.2. Full Scale Testing

Fatigue life assessment of components working in an H₂ environment is one of the topics of interest, for compressed H₂ storage vessels that undergo pressure cycling during operation. The actual fatigue assessment of similar components is based on fracture mechanics models, but there are conflicting opinions regarding the predictive capabilities of the models with respect to the test results, a sign that the topic must be further investigated. San Marchi et al. [58,59] and Yamabe et al. [60,61] performed H₂ full-scale cycling tests of pre-notched CrMo pressure vessels at 45 MPa and they demonstrated that the number of cycles to the failure found experimentally was higher than predicted by fracture mechanics design methods. On the contrary, de Miguel et al. [62] showed as the number of cycles before the break was lesser than predicted by calculation and they attributed the differences to several parameters, such as cycling frequency, notch geometry, and crack morphology. Consequently, it is evident that the topic must be further investigated and that there is not a univocal testing procedure to address this issue. First pressure cycling full-scale tests in the ΔH lab were performed to start investigating this issue. A preliminary test was performed

cycling an internally pre-notched AISI 4145 vessel (see Figure 8a) between 5 and 45 MPa for 3500 cycles.

The post-test analysis does not highlight any crack propagation in correspondence to the two notched areas (see Figure 8b), showing that this type of vessel can withstand a much higher number of cycles, as reported by San Marchi et al. [58,59] and Yamabe et al. [59] on Cr-Mo steel pressure vessels. This preliminary test allowed to verify the suitability of the testing procedure and to obtain a first result. Further activities are planned to continue the investigations.

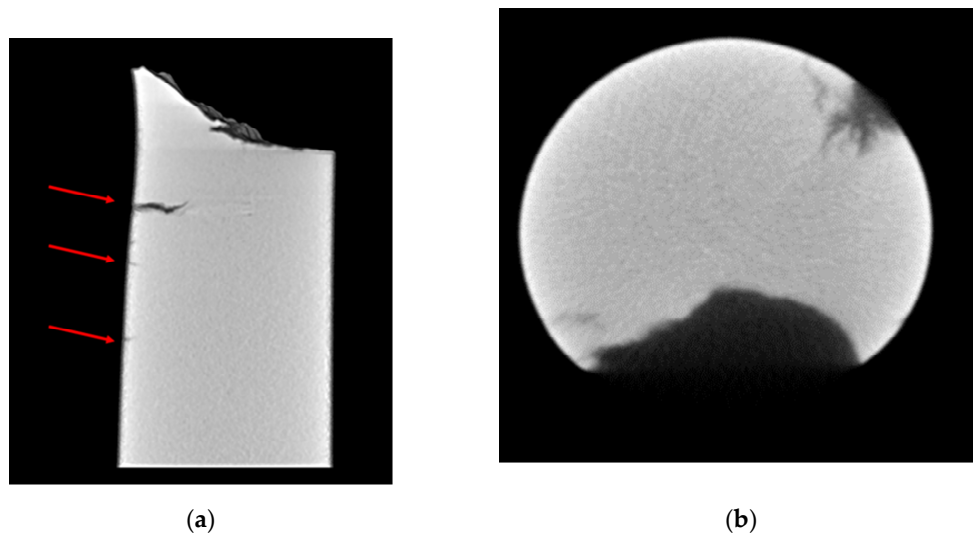


Figure 7. (a) μ Tomo 3D reconstruction of tomographic vertical cut of specimen in H_2 . The red arrows point to the cracks propagating from the outer surface; (b) μ Tomo 3D reconstruction of tomographic cut of specimen in H_2 showing the internal structure of the cracks.

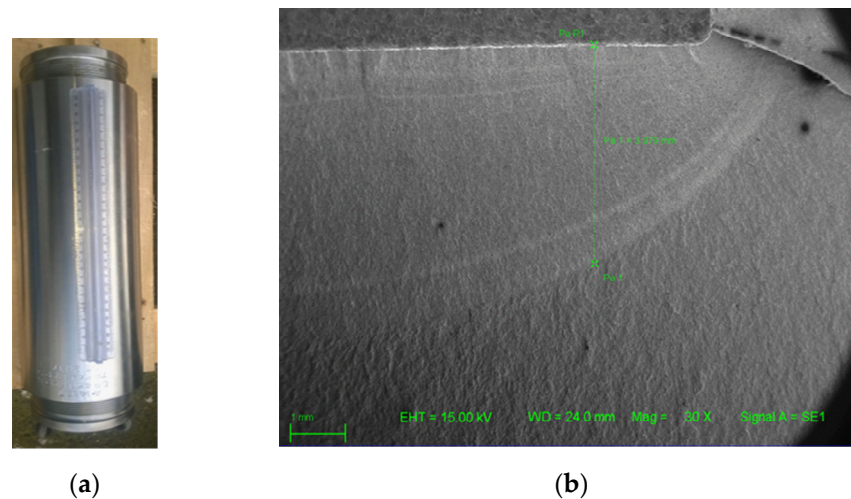


Figure 8. (a) AISI 4145 Vessel; (b) SEM micrograph of the fracture zone—fatigue test in H_2 .

5.3. Hydrogen Adsorption at High Pressures

The evaluation of H_2 adsorption in tanks with a volume on the liter range was allowed using the HPcT apparatus. A reference test was carried out by comparing the amount of H_2 that, under the same pressure and temperature conditions, was introduced into a reservoir with a fixed volume. The test was performed by a direct comparison between cGH₂ (empty 1-liter reservoir) method and the SSMs-Physisorption (1-liter reservoir containing 512 g of activated carbon NUCHAR SA-20[®]) one.

Figure 9a,b show the variation in pressure and temperature (T1 environment, T2 delivery pipe, T3 reservoir) vs. time when a fixed H₂ flux (50 liters STP/min) was delivered to the reservoir.

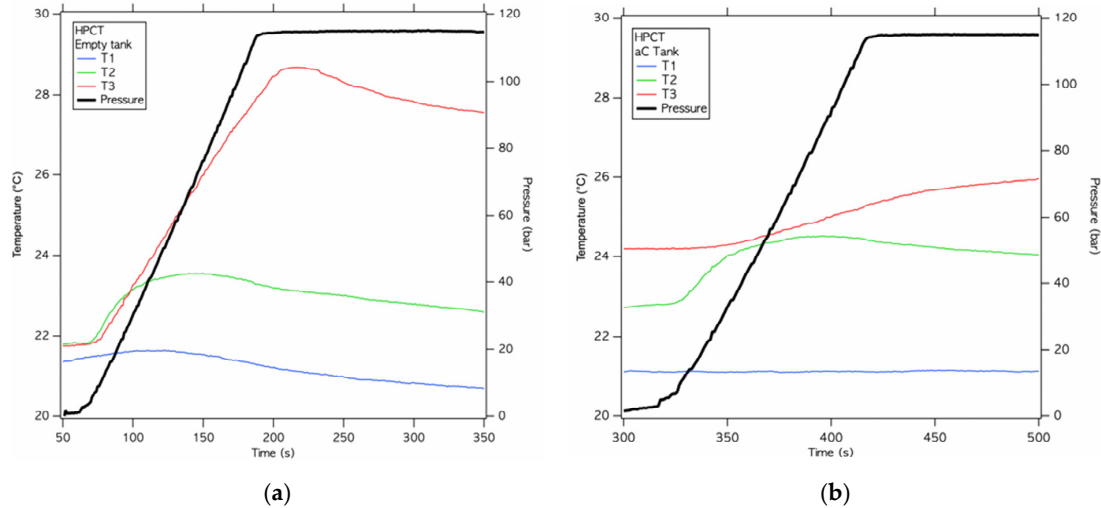


Figure 9. (a) H₂ adsorption on active carbon NUCHAR SA. H₂ pressure and temperatures for a 1-liter reservoir filled with a constant 50 STP liters/min flow in empty reservoir; (b) H₂ adsorption on active carbon NUCHAR SA. H₂ pressure and temperatures for a 1-liter reservoir filled with a constant 50 STP liters/min flow in SSM-filled reservoir.

This allowed to directly compare the net increase of H₂ stored in the reservoir due to the presence of adsorbing material (Figure 10a). As it can be noted in the figure, the presence of the SSM results in a storage gain all over the pressure range with the highest increase, equal to 26%, observed at 12 MPa. The behavior of the adsorbing material is fully reversible over several adsorption/desorption cycles (results not shown). For the sake of comparison, we evaluated the H₂ net adsorption by the SSM powder from the data presented in Figure 10b. By considering the volume occupied by the activated carbon, whose skeletal density is 1.95 g/cc [49], we evaluated the net adsorption in the 0–120 bar range and represented it in Figure 10b as an isotherm adsorption curve. The result is in strict agreement with previous studies performed on mg-scale quantities [49] where the same material was tested up to 80 bar.

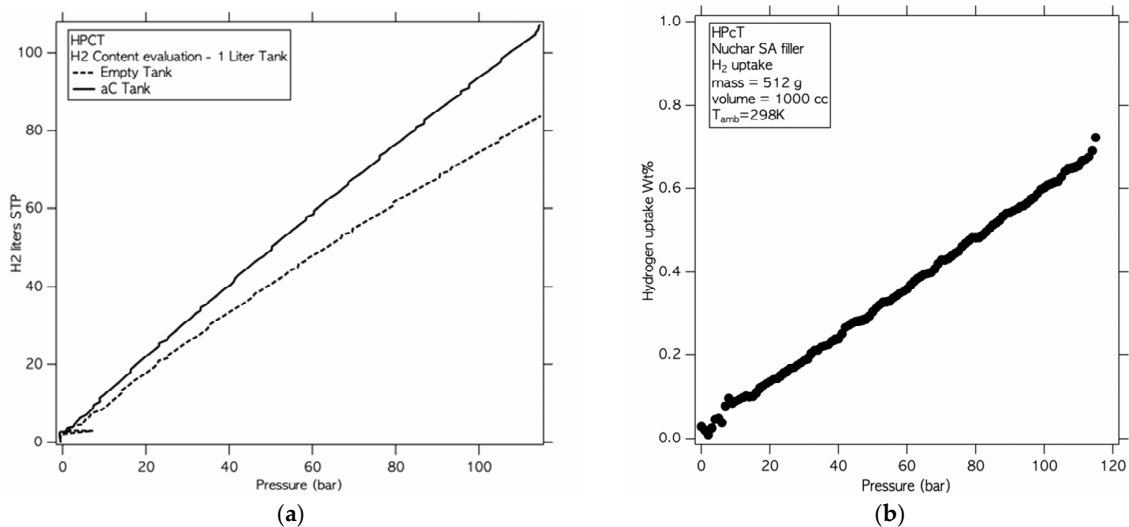


Figure 10. (a) Comparison of the stored hydrogen mass in the 0–12 MPa range (see text): absolute quantities uptake by the SSM powder; (b) Comparison of the stored hydrogen mass in the 0–12 MPa range (see text): net hydrogen uptake by the SSM powder.

6. Conclusions

Hydrogen as an energy carrier is becoming more and more interesting in carbon footprint reduction in Europe. There are several technologies for H₂ storage, characterized by pros and cons that make each of them attractive for a specific scenario. In any case, the challenge to get materials and components suitable to work in an H₂ environment, guaranteeing safety and reliability, is an important issue. In this context, the work highlights some storage techniques and their correlation with materials properties, showing the necessity of a multidisciplinary approach to the study of H₂ storage and distribution. In this frame, preliminary tests were performed in a specific lab, devoted to test and characterize material and components for H₂ storage and transportation in relevant environment, in terms of pressure and temperature.

The first test campaign highlights the following results:

- The slow strain rate tests show an evident H₂ effect on elongation and surface fracture of the material. The sample tested at 80 MPa in an inert environment has an elongation almost double with respect to the sample tested in H₂. The scanning electron micrographs confirm a fracture surface characterized by a predominant brittle propagation mode (both transgranular and intergranular) and the presence of secondary crack for the sample tested in an H₂ environment, such as highlighted by micro-tomography analysis.
- The fatigue full-scale test performed in an H₂ environment confirm the good performance of AISI 4145 alloy in a high-pressure regime at low pressure range. In fact, after being exposed to H₂ pressure with a pre-machined notch, undergoing severe fatigue cycles, there is no evidence of fatigue crack propagation, as showed by scanning electron microscopy.
- The test on solid state materials shows as the presence of the adsorbed material results in a storage gain all over the pressure range with the highest increase, equal to 26%, observed at 12 MPa, which is in agreement with previous studies performed on NUCHAR SA in mg-scale quantities. This result highlight as the prototype is able to evaluate the adsorption capacity of solid-state materials on Kg-scale quantities obtaining results comparable to laboratory scale results.

In conclusion, the work shows that the critical point for the H₂ economy development is the selection of the suitable storage method for a specific application, the materials compatibility with gas and the necessity of an integrated multidisciplinary approach to these issues.

Author Contributions: Conceptualization, S.S. and R.G.A. and E.M.; validation, E.M. and R.G.A.; formal analysis, R.F. and S.S.; investigation, A.R. and R.F. and G.C.; resources, S.S. and A.P. and L.P.; data curation, S.S.; writing—original draft preparation, S.S.; writing—review and editing, R.G.A. and E.M.; visualization, S.S.; supervision, R.G.A. and V.F. and L.D.V.; project administration, L.D.V. and A.R.; All authors have read and agreed to the published version of the manuscript.

Funding: This research received no external funding.

Institutional Review Board Statement: Not applicable.

Informed Consent Statement: Informed consent was obtained from all subjects involved in the study.

Data Availability Statement: Data is contained within the article.

Conflicts of Interest: The authors declare no conflict of interest.

References

1. European Parliament. European Parliament Directive (EU) 2018/2001 of the European Parliament and of the Council of 11 December 2018 on the promotion of the use of energy from renewable sources (recast). *Off. J. Eur. Union* **2018**, *2018*, 82–207.
2. Aneke, M.; Wang, M.E. Energy storage technologies and real-life applications—a state of the art review. *Appl. Energy* **2016**, *179*, 350–377. [[CrossRef](#)]
3. Koohi-Fayegh, S.; Rosen, M.A. A review of energy storage types, applications and recent developments. *J. Energy Storage* **2020**, *27*, 101047. [[CrossRef](#)]

4. IRENA International Renewable Energy Agency. *Hydrogen from Renewable Power: Technology Outlook for the Energy Transition*; International Renewable Energy Agency: Abu Dhabi, United Arab Emirates, 2018.
5. Staffell, I.; Scamman, D.; Abad, A.V.; Balcombe, P.; Dodds, P.E.; Ekins, P. The role of hydrogen and fuel cells in the global energy system. *Energy Environ. Sci.* **2019**, *12*, 157E. [CrossRef]
6. Glenk, G.; Reichelstein, S. Economics of converting renewable power to hydrogen. *Nat. Energy* **2019**, *4*, 216–222. [CrossRef]
7. Maggio, G.; Nicita, A.; Squadrito, G. How the hydrogen production from RES could change energy and fuel markets: A review of recent literature. *Int. J. Hydrog. Energy* **2019**, *44*, 11371–11384. [CrossRef]
8. Petreanu, I.; Dragan, M.; Badea, S.L. *Fuel Cells: Alternative Energy Sources for Stationary, Mobile and Automotive Applications*; Vizureanu, P., Ed.; IntechOpen: London, UK, 2020. [CrossRef]
9. Jayakumar, A.; Chalmers, A.; Lie, T.T. Review of prospects for adoption of fuel cell electric vehicles in New Zealand. *IET Electr. Syst. Transp.* **2017**, *7*, 259–266. [CrossRef]
10. Khzouz, M.I.; Gkanas, E.I. *Hydrogen Technologies for Mobility and Stationary Applications: Hydrogen Production, Storage and Infrastructure Development, Renewable Energy—Resources, Challenges and Applications*; Qubeissi, M.A., El-kharouf, A., Soyhan, H.S., Eds.; IntechOpen: London, UK, 2020. [CrossRef]
11. Hydrogen Cars All Models at a Glance. Available online: <https://h2.live/en/wasserstoffautos> (accessed on 26 March 2021).
12. Abdallaa, A.M.; Hossaina, S.; Nisfindya, O.B.; Azadd, A.T.; Dawood, M.; Azada, A.K. Hydrogen production, storage, transportation and key challenges with applications: A review. *Energy. Convers. Manag.* **2018**, *165*, 602–627. [CrossRef]
13. IEA International Energy Agency. *The Future of Hydrogen*; International Energy Agency: Paris, France, 2019.
14. Azzaro-Pantel, C. Hydrogen Supply Chain: Design, Deployment and Operation. 2018. Available online: <https://search.ebscohost.com/login.aspx?direct=true&scope=site&db=nlebk&db=nlabk&AN=1649248> (accessed on 26 March 2021).
15. Liu, W.; Sun, L.; Li, Z. Trends and future challenges in hydrogen production and storage research. *Environ. Sci. Pollut. Res.* **2020**, *27*, 31092–31104. [CrossRef]
16. Peschel, A. Industrial Perspective on Hydrogen Purification, Compression, Storage, and Distribution. *Fuel Cells* **2020**, *20*. [CrossRef]
17. Abe, J.O.; Popoola, A.P.I.; Ajenifuja, E.; Popoola, O.M. Hydrogen energy, economy and storage: Review and recommendation. *Int. J. Hydrog. Energy* **2019**, *44*, 15072–15086. [CrossRef]
18. Klebanoff, L. *Hydrogen Storage Technology: Materials and Applications*, 1st ed.; CRC Press: New York, NY, USA, 2016.
19. Zhang, S.; Lee, L.H.; Sun, Y.; Liu, Y. Materials for Hydrogen Mobile Storage Applications. *IOP Conf. Ser. Earth Environ. Sci.* **2021**, *632*, 052087. [CrossRef]
20. Zuttel, A. Hydrogen storage methods. *Naturwissenschaften* **2004**, *91*, 157–172. [CrossRef]
21. Pethaiah, S.S.; Sadasivuni, K.K.; Jayakumar, A.; Ponnamma, D.; Tiwary, C.S.B.; Sasikumar, G. Methanol Electrolysis for Hydrogen Production Using Polymer Electrolyte Membrane: A Mini-Review. *Energies* **2020**, *13*, 5879. [CrossRef]
22. Boateng, E.; Chen, A. Recent advances in nanomaterial-based solid-state hydrogen storage. *Mater. Today Adv.* **2020**, *6*, 100022. [CrossRef]
23. Modisha, P.M.; Ouma, C.N.M.; Garidzirai, R.; Wasserscheid, P.; Bessarabov, D. The Prospect of Hydrogen Storage Using Liquid Organic Hydrogen Carriers. *Energy Fuels* **2019**, *33*, 2778–2796. [CrossRef]
24. Robertson, I.M.; Sofronis, P.; Nagao, A.; Martin, M.L.; Wang, S.; Gross, D.W. Hydrogen Embrittlement Understood. *Metall. Mater. Trans. B* **2015**, *46*, 10851103. [CrossRef]
25. Eguch, K.; Burnett, T.L.; Engelberg, D.L. X-Ray tomographic characterisation of pitting corrosion in lean duplex stainless steel. *Corros. Sci.* **2020**, *165*, 108406. [CrossRef]
26. Wu, K.; Ito, K.; Shinozaki, I.; Chivavibul, P.; Enoki, M. A Comparative Study of Localized Corrosion and Stress Corrosion Cracking of 13Cr Martensitic Stainless Steel Using Acoustic Emission and X-ray Computed Tomography. *Materials* **2019**, *12*, 2569. [CrossRef]
27. Laquai, R.; Schaupp, T.; Müller, B.R.; Griesche, A.; Kupsch, A.; Lange, A. 3D Crack Analysis in Hydrogen Charged Lean Duplex Stainless Steel with Synchrotron Refraction CT. In Proceedings of the 19th World Conference on Non-Destructive Testing 2016, Munich, Germany, 13–17 June 2016.
28. Dong, Z.; Zhang, X.; Shi, W.; Zhou, H.; Lei, H.; Liang, J. Study of Size Effect on Microstructure and Mechanical Properties of AlSi10Mg Samples Made by Selective Laser Melting. *Materials* **2018**, *11*, 2463. [CrossRef]
29. Rouquerol, J.; Avnir, D.; Fairbridge, C.W.; Everett, D.H.; Haynes, J.M.; Pernicone, N.; Ramsay, J.D.F.; Sing, K.S.W.; Unger, K.K. Recommendations for the characterization of porous solids (Technical Report). *Pure Appl. Chem.* **1994**, 1739. [CrossRef]
30. Rouquerol, F.; Rouquerol, J.; Sing, K. Adsorption by Powders and Porous Solids Principles, Methodology and Applications. *Sci. Direct* **2012**, *2*, 646.
31. Zuttel, A. Materials for hydrogen storage. *Mater. Today* **2003**, *6*, 24–33. [CrossRef]
32. Barthelemy, H.; Weber, M.; Barbier, F. Hydrogen storage: Recent improvements and industrial perspectives. *Int. J. Hydrog. Energy* **2017**, *42*, 7254–7262. [CrossRef]
33. Rivard, E.; Trudeau, M.; Zaghbi, K. Hydrogen Storage for Mobility: A Review. *Materials* **2019**, *12*, 1973. [CrossRef]
34. Nagumo, M. *Fundamental of Hydrogen Embrittlement*; Springer: Singapore, 2016.
35. Dwivedi, S.K.; Vishwakarma, M. Hydrogen embrittlement in different materials: A Review. *Int. J. Hydrog. Energy* **2018**, *43*, 21603–21616. [CrossRef]

36. Atrens, A.; Liu, Q.; Tapia-Bastidas, C.; Gray, E.; Irwanto, B.; Venezuela, J.; Liu, Q. Influence of Hydrogen on Steel Components for Clean Energy. *Corros. Mater. Degrad.* **2020**, *1*, 2. [CrossRef]
37. Li, M.; Bai, Y.; Zhang, C.; Song, Y.; Jiang, S.; Grouset, D.; Zhang, M. Review on the research of hydrogen storage system fast refueling in fuel cell vehicle. *Int. J. Hydrog. Energy* **2019**, *44*, 10677–10693. [CrossRef]
38. Yanxing, Z.; Maoqiong, G.; Yuan, Z.; Xueqiang, D.; Jun, S. Thermodynamics analysis of hydrogen storage based on compressed gaseous hydrogen, liquid hydrogen and cryo-compressed hydrogen. *Int. J. Hydrog. Energy* **2019**, *44*, 16833–16840. [CrossRef]
39. Langmi, H.W.; Ren, J.; North, B.; Mathe, M.; Bessarabov, D. Hydrogen Storage in Metal-Organic Frameworks: A Review. *Electrochim. Acta* **2014**, *128*, 368–392. [CrossRef]
40. Anderson, P.A. Storage of hydrogen in zeolites. In *Solid-State Hydrogen Storage*; Woodhead Publishing: Cambridge, UK, 2008; pp. 223–260.
41. Von Colbe, B.J.; Ares, J.R.; Barale, J.; Baricco, M.; Buckley, C.; Capurso, G.; Gallandat, N.; Grant, D.M.; Guzik, M.N.; Jacob, I.; et al. Application of hydrides in hydrogen storage and compression: Achievements, outlook and perspectives. *Int. J. Hydrog. Energy* **2019**, *44*, 7780–7808. [CrossRef]
42. Tian, M.; Rochat, S.; Polak-Krašna, K.; Holyfield, L.T.; Burrows, A.D.; Bowen, C.R.; Mays, T.J. Nanoporous polymer-based composites for enhanced hydrogen storage. *Adsorption* **2019**, *25*, 889–901. [CrossRef]
43. Liu, B.; Xiao, J.; Xu, L.; Yao, Y.; Costa, B.F.O.; Domingos, V.F.; Ribeiro, E.S.; Shi, F.N.; Zhou, K.; Su, J.; et al. Gelatin-assisted sol-gel derived TiO₂ microspheres for hydrogen storage. *Int. J. Hydrog. Energy* **2015**, *40*, 4945–4950. [CrossRef]
44. Stelitano, S.; Conte, G.; Policicchio, A.; Aloise, A.; Desiderio, G.; Agostino, R.G. Pinecone-Derived Activated Carbons as an Effective Medium for Hydrogen Storage. *Energies* **2020**, *13*, 2237. [CrossRef]
45. Hirscher, M.; Yartys, V.A.; Baricco, M.; von Colbe, J.B.; Blanchard, D.; Bowman, R.C.; Broom, D.P.; Buckley, C.E.; Chang, F.; Chen, P.; et al. Materials for hydrogen-based energy storage—Past, recent progress and future outlook. *J. Alloy Compd.* **2020**, 827. [CrossRef]
46. Niaz, S.; Manzoor, T.; Pandith, A.H. Hydrogen storage: Materials, methods and perspectives. *Renew. Sust. Energy Rev.* **2015**, *50*, 457–469. [CrossRef]
47. Ren, J.; Musyok, N.M.; Langmi, H.W.; Mathe, M.; Liao, S. Current research trends and perspectives on materials-based hydrogen storage solutions: A critical review. *Int. J. Hydrog. Energy* **2017**, *42*, 289–311. [CrossRef]
48. EOMAT Sistemi e Materiali Innovativi per la Produzione e Stoccaggio di Energia Rinnovabile PON03PE_00092_1. Available online: <http://www.ponrec.it/open-data/progetti/scheda-progetto?ProgettoID=7350> (accessed on 2 April 2021).
49. Minuto, F.D.; Policicchio, A.; Aloise, A.; Agostino, R.G. Liquid-like hydrogen in the micropores of commercial activated carbons. *Int. J. Hydrog. Energy* **2015**, *40*, 14562–14572. [CrossRef]
50. Ugiansky, G.M.; Payer, J.H. *ASTM STP 665: Stress Corrosion Cracking: The Slow Strain-Rate Technique*; ASTM International: West Conshohocken, PA, USA, 1979.
51. Kane, R.D. *Slow Strain Rate Testing for the Evaluation of Environmentally Induced Cracking: Research and Engineering Applications*; ASTM International: West Conshohocken, PA, USA, 1993.
52. Martinez-Paneda, E.; Harris, Z.D.; Fuentes-Alonso, S.; Scully, J.R.; Burns, J.T. On the suitability of slow strain rate tensile testing for assessing hydrogen embrittlement susceptibility. *Corros. Sci.* **2020**, *163*, 108291. [CrossRef]
53. Matsunaga, H. Slow strain rate tensile and fatigue properties of Cr-Mo and carbon steels in a 115 MPa hydrogen gas atmosphere. *Int. J. Hydrog. Energy* **2015**, *40*, 5739–5748. [CrossRef]
54. Briottet, L.; Moro, I.; Lemoine, P. Quantifying the Hydrogen Embrittlement of Pipe Steels for Safety Considerations. *Int. J. Hydrog. Energy* **2012**, *37*, 17616–17623. [CrossRef]
55. Yamabe, J.; Takakuwa, O.; Matsunaga, H.; Itoga, H.; Matsuoka, S. Hydrogen diffusivity and tensile-ductility loss of solution-treated austenitic stainless steels with external and internal hydrogen. *Int. J. Hydrog. Energy* **2017**, *42*, 13289–13299. [CrossRef]
56. Matsuoka, S.; Yamabe, J.; Matsunaga, H. Criteria for determining hydrogen compatibility and the mechanisms for hydrogen-assisted, surface crack growth in austenitic stainless steels. *Eng. Fract. Mech.* **2016**, *153*, 103–127. [CrossRef]
57. Matsuoka, S.; Yamabe, J.; Matsunaga, H. Mechanism of Hydrogen-Assisted Surface Crack Growth of Austenitic Stainless Steels in Slow Strain Rate Tensile Test. In Proceedings of the ASME Pressure Vessels and Piping Conference PVP2016-63394, Vancouver, BC, Canada, 17–21 July 2016. [CrossRef]
58. San Marchi, C.; Dedrick, D.E.; Van Blarigan, P.; Somerday, B.P.; Nibur, K. *Pressure Cycling of Type 1 Pressure Vessels with Gaseous Hydrogen*; ICHS: San Francisco, CA, USA, 2011.
59. San Marchi, C.; Harris, A.; Yip, M.; Somerday, B.P.; Nibur, K. Pressure Cycling of Steel Pressure Vessels with Gaseous Hydrogen. In Proceedings of the ASME Pressure Vessels & Piping Conference PVP2012, Toronto, ON, Canada, 15–19 July 2012; pp. 835–844. [CrossRef]
60. Yamabe, J.; Itoga, H.; Awane, T.; Matsunaga, H.; Hamada, S.; Matsuoka, S. Fatigue-life and Leak-Before-Break Assessments of Cr-Mo Steel Pressure Vessels with High-Pressure Gaseous Hydrogen. In Proceedings of the ASME 2014 Pressure Vessels & Piping Conference PVP2014, Anaheim, CA, USA, 20–24 July 2014; p. 28604. [CrossRef]
61. Yamabe, J.; Itoga, H.; Awane, T.; Matsuo, T.; Matsunaga, H.; Matsuoka, S. Pressure cycle testing of Cr-Mo steel pressure vessels subjected to gaseous hydrogen. *J. Press. Vessel Technol.* **2015**, *138*, 011401. [CrossRef]
62. De Miguel, N.; Acosta, B.; Moretto, P.; Briottet, L.; Bortot, P.; Mecozzi, E. Hydrogen enhanced fatigue in full scale metallic vessel tests—Results from the MATHRYCE project. *Int. J. Hydrog. Energy* **2017**, *42*, 13777–13788. [CrossRef]